

# Density-functional calculation of Landau levels for quasi-two-dimensional hole gases

W. O. G. Schmitt

*Physikalisches Institut, Am Hubland, D-97074 Würzburg, Federal Republic of Germany*

(Received 27 July 1994)

*p*-type accumulation and inversion layers at a [110] Si surface in large external magnetic fields are investigated in the Sham-Kohn approximation. We consider the magnetic field dependence of the self-consistent potential for up to two occupied subbands. The transversal resistivity is calculated in the self-consistent Born approximation and compared with the density of states in the lowest order cumulant approximation. Some features of the Shubnikov-de Haas effect, i.e., the beating pattern for the case of one occupied subband and the second oscillation, which appears when one further subband is populated, could be reproduced quantitatively. The dependence of the node in the beating pattern on an externally applied uniaxial strain is explained qualitatively.

## I. INTRODUCTION

During the last decades two-dimensional (2D) electronic systems at semiconductor surfaces or interfaces have been intensively studied. Due to a strong electric field perpendicular to the surface, there are bound states, which result in electrical subbands because of the translational symmetry in directions parallel to the surface. Silicon-metal-oxide-semiconductor field-effect transistors<sup>1</sup> (MOSFET's) have been popular for studying many-body effects in quasi-two-dimensional Fermi gases, as (1) these effects are especially large in Si (Ref. 2) because of its material parameters (masses and dielectric constant) and because (2) the particle density can be controlled by an external gate voltage over several orders of magnitude.

As to *p*-type inversion layers, the first systematic experiments to be done were measurements of the Shubnikov-de Haas effect.<sup>3-5</sup> An early theoretical success was the explanation of cyclotron masses, which were extracted semiclassically from self-consistent  $\mathbf{k} \cdot \mathbf{p}$ -subband calculations in Hartree approximation for a vanishing magnetic field.<sup>6</sup> However, since for hole gas systems described by Luttinger's matrix<sup>7,8</sup> the motion parallel and perpendicular to the surface is coupled, the Landau level spectrum generally cannot be inferred from the subband dispersion but has to be calculated self-consistently by introducing the magnetic field in Peierls' approximation.<sup>9</sup>

Although many-body effects are important, calculations for *p*-type systems like Si MOSFET's,<sup>10-12</sup> GaAs-Ga<sub>x</sub>Al<sub>1-x</sub>As heterostructures,<sup>13-16</sup> or Ge bicrystals<sup>9</sup> are done only in Hartree approximation because of the complicated valence band structure of the bulk material. Recently, we showed<sup>17</sup> how exchange and correlation effects could be allowed for easily by adopting the Sham-Kohn<sup>18</sup> approach, which was applied to *n*-type Si MOSFET's by Ando.<sup>19</sup> The approximation we and Ando used is formally almost equivalent to the density-functional approach of Hohenberg, Kohn, and Sham<sup>20-22</sup> in the local-density approximation. Finite external magnetic fields might require a generalization to a current- and spin-

density-functional formalism.<sup>23</sup> However, in the following we will use the same exchange-correlation potential as for the  $B = 0$  case because (1) the corresponding functionals for  $B \neq 0$  are not known for our system and because (2) we expect differences between the  $B = 0$  and the  $B \neq 0$  formalism to be small as long as the system is far from the magnetic quantum limit. This conjecture is supported by the Hartree potential being almost independent of  $\mathbf{B}$  as long as several Landau levels are occupied (at least when only one subband is populated).

In Sec. II, we outline how the Landau levels of *p*-type accumulation or inversion layers at a Si-[110] surface can be determined. Here, we are interested in how much the potential is dependent on the magnetic field. Afterwards we calculate the Shubnikov-de Haas effect (Sec. III), i.e., the transversal resistivity for this system in the self-consistent Born approximation (SCBA) and compare it with the density of states at the Fermi edge in the lowest order cumulant approximation (LOCA). By this we study the beating pattern in the magnetoquantum oscillations, which has been discovered by von Klitzing *et al.*<sup>3</sup> and investigated in detail by Dorozhkin and Ol'shanetskii.<sup>24,25</sup> Furthermore, we are interested in the Shubnikov-de Haas effect for two occupied subbands which is an indirect means for examining subband energy separations. Finally, we investigate the Shubnikov-de Haas effect under an external uniaxial stress and compare it with recent experiments of Dorozhkin.<sup>26</sup>

## II. SELF-CONSISTENT LANDAU LEVELS

In this section, we outline how Landau levels of *p*-type accumulation and inversion layers at a [110]-Si surface can be calculated self-consistently. We choose  $R_0 = e^2 m_0 / (2(4\pi\epsilon_0)^2 \hbar^2 e^2 \gamma_1)$ ,  $a_0 = \epsilon \gamma_1 \times 4\pi\epsilon_0 \hbar^2 / (e^2 m_0)$ ,  $\beta_0 = R_0 / (\gamma_1 \mu_B)$  as units of energy, length, and magnetic field and we invert the energy scale. The kinetic energy operator  $H_L(\mathbf{k}', \mathbf{B}, \epsilon_{\mu\nu})$  for a finite external magnetic field  $\mathbf{B}$  and strain tensor  $\epsilon_{\mu\nu}$  is given in the Appendix. Here

$\mathbf{k}' = \mathbf{k} + \mathbf{A}$  is the kinematical momentum ( $\mathbf{A} =$  vector potential,  $\mathbf{B} = \nabla \times \mathbf{A}$ ), which satisfies the gauge invariant commutation relation

$$\mathbf{k}' \times \mathbf{k}' = -2i\mathbf{B}. \quad (1)$$

For  $\mathbf{B} = (0, 0, B)$ , it is convenient to define the operators

$$a = (k'_x - ik'_y)l/\sqrt{2}, \quad (2a)$$

$$a^\dagger = (k'_x + ik'_y)l/\sqrt{2}, \quad (2b)$$

with the magnetic length  $l = (2B)^{-1/2}$ . Equation (1) results in  $[a, a^\dagger] = 1$  and thus we find for the eigenstates  $|n\rangle$  of the number operator  $N = a^\dagger a$ ,

$$a|n\rangle = \sqrt{n}|n-1\rangle, \quad (3a)$$

$$a^\dagger|n\rangle = \sqrt{n+1}|n+1\rangle. \quad (3b)$$

In the Appendix,  $H_L$  has been expressed by  $a$ ,  $a^\dagger$ ,  $N$ , and  $k_z = i\partial/\partial z$ . With this the differential equation to be solved runs

$$[H_L(a, a^\dagger, k_z, B, \varepsilon_{\nu\mu}) + v(z)]\zeta(z) = E\zeta(z), \quad (4)$$

with  $\zeta(z) \rightarrow 0$  for  $z \rightarrow 0$  or  $z \rightarrow \infty$  ( $z$  measures the distance from the surface) and  $v(z)$  being the sum of an image ( $8\pi(\varepsilon - \varepsilon')/[(\varepsilon + \varepsilon')4z]$ ,  $\varepsilon' =$  dielectric constant of the oxide), depletion ( $8\pi N_d z_d z$ ,  $N_d =$  effective doping concentration,  $z_d =$  depletion length), Hartree [ $8\pi \int_z^\infty dz'(z - z')n(z')$ ,  $n =$  density of holes], and exchange-correlation potential, the latter in Sham-Kohn approximation.<sup>17</sup>

When we choose the Landau gauge  $\mathbf{A} = (0, Bx, 0)$ ,  $H$  and  $N$  commute with the center of coordinate operator  $X = -l^2 k_y$ . The wave functions  $\zeta$  are expanded in eigenstates  $|n\rangle$  of  $N$  and  $X$  (the quantum number  $X$  being dropped):

$$\zeta_{qj}(z) = \sum_{n=0}^{\infty} \begin{pmatrix} \zeta_{qjn}^{(0)} |n_{q0}\rangle \\ \zeta_{qjn}^{(1)} |n_{q1}\rangle \\ \zeta_{qjn}^{(2)} |n_{q2}\rangle \\ \zeta_{qjn}^{(3)} |n_{q3}\rangle \\ \zeta_{qjn}^{(5)} |n_{q5}\rangle \\ \zeta_{qjn}^{(4)} |n_{q4}\rangle \end{pmatrix}, \quad (5)$$

with  $q = 0, 1$  and

$$|n_{q\alpha}\rangle = \begin{cases} 2n & \text{for } q + \alpha \text{ even} \\ 2n + 1 & \text{for } q + \alpha \text{ odd.} \end{cases}$$

We found that it is sufficient to restrict the sum to  $n_{\max} = 6 + \eta/2$  terms in order to get the occupied levels accurately enough for the subsequent analysis, where  $\eta = 2\pi l^2 N_h$  is the filling factor and  $N_h$  the surface density of the holes.

For calculating the Hartree and the exchange-

correlation potential, we need the density

$$n(z) = \frac{1}{2\pi l^2} \sum_{qj\alpha} |\zeta_{qjn}^{(\alpha)}(z)|^2 \Theta(\mu - E_{qj}).$$

Inserting ansatz (5) in (4) and making use of (3), we find a system of  $(36 + 3\eta)$  coupled differential equations, the numerical solution of which has been described in Refs. 9 and 17.

For the parameters,<sup>17</sup> we use the values  $\gamma_1 = 4.17$ ,  $\gamma_2 = 0.45$ ,  $\gamma_3 = 1.36$ ,  $\varepsilon = 11.7$ , and  $\varepsilon' = 3.7$ .

For the case of only *one* occupied subband ( $N_h = 2 \times 10^{12} \text{ cm}^{-2}$ ,  $N_d = 10^{15} \text{ cm}^{-3}$ ), Fig. 1(a) shows the Landau level spectrum, i.e., the difference of a Landau level and the lowest one. Solid (dotted) lines correspond to the solutions for  $q = 0$  ( $q = 1$ ). Vertical lines indicate where the Fermi energy jumps from one Landau level to the next one at integer filling factors. At  $\eta = 9.5$ , the levels are labeled by quantum numbers: the first two subbands are heavy hole bands ( $h$ ),  $\pm$  gives the "spin polarization," and the last number is the Landau quantum number of the largest integral  $\int dz \sum_{\alpha} |\zeta_{qjn}^{(\alpha)}|^2$ . Of course, the quantum numbers are only approximate and the worse defined the higher excited the level of a considered subband is. Anticrossing occurs for levels with the same exact quantum number  $q$ .

The Landau fan Fig. 1(a) has three peculiar properties: (1) The higher excited a level is the more it is curved. However, this effect is much smaller than, e.g., in Ge, which can be understood easily by comparing the effective unit  $\beta_0$ , which is 5.5 T in Ge and 100 T in Si. Thus  $B=10$  T is a much smaller perturbing field in Si ( $B/\beta_0 = 0.1$ ) than in Ge ( $B/\beta_0 = 1.8$ ). (2) A description of the Landau plot by  $g$  factors is not possible: For example, the levels  $h\pm, 5$  have a "spin splitting" smaller than half the level distance for  $B = 2.5$  T and a much larger splitting for  $B = 9$  T. (3) For  $B = \text{const}$ , the levels  $h\pm, n$  change the order: For  $B = 2.5$  T the 27th and the 28th level have about the same energy.

Figure 1(b) corresponds to the same system but higher magnetic fields. The solid lines refer to a full (i.e., for every  $\eta$ ) self-consistent calculation and the dotted lines to a calculation with a potential  $v(z)$ , that has been determined self-consistently for  $\eta_0 = 9.5$ . Significant differences occur only in the magnetic quantum limit  $\eta \lesssim 1$ . For  $\eta > 2$ , the potential  $v(z)$  approximately is independent of  $\eta$ .

As soon as a second subband is occupied, we observe a different behavior. Figure 2(a) shows the Landau spectrum for  $N_h = 8 \times 10^{12} \text{ cm}^{-2}$ ,  $N_d = 10^{15} \text{ cm}^{-3}$ , and a potential  $v(z)$  determined for  $\eta_0 = 9.5$ , which has to be compared with the full self-consistent spectrum in Fig. 2(b). In the latter there are discontinuities in the derivative of a level, when the Fermi energy jumps from a steep level belonging to the ground subband to a flat level belonging to the first excited subband. The reason is that the envelope functions for different subbands have a different  $z$  dependence. According to the results for merely one occupied subband, we expect the normalized density of the  $\nu$ th subband,

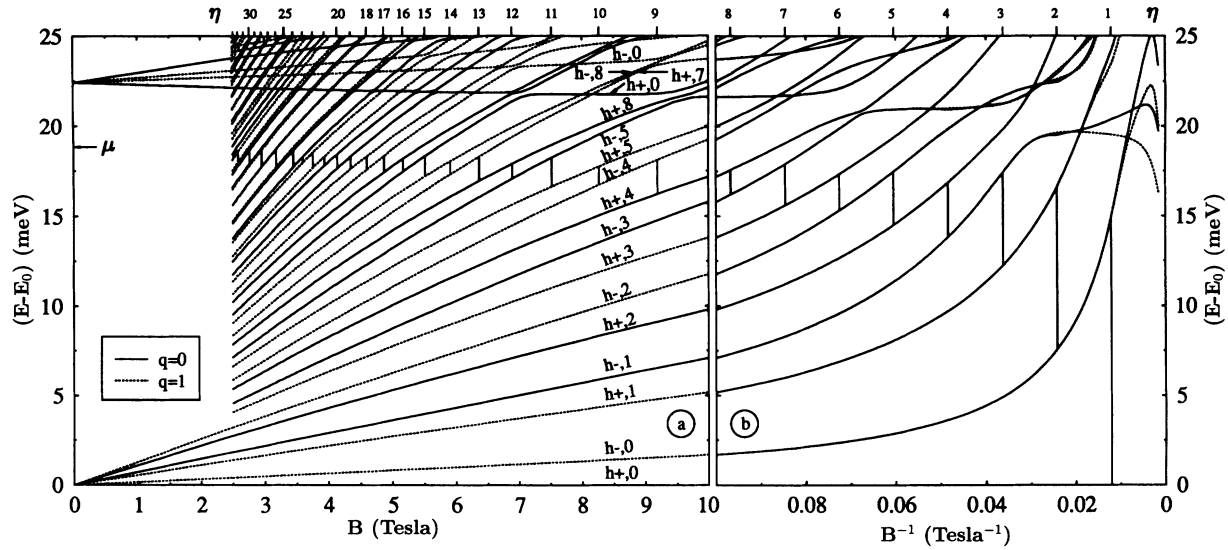


FIG. 1. Difference of Landau levels and the lowest level as a function of  $B$  for an inversion layer with one occupied subband ( $N_h = 2 \times 10^{12} \text{ cm}^{-2}$ ,  $N_d = 10^{15} \text{ cm}^{-3}$ ). In this plot the Fermi energy  $\mu$  is not constant but jumps at integer filling factors from the highest occupied to the lowest unoccupied level. (a) Solid (dotted) lines refer to solutions with  $q = 0$  ( $q = 1$ ). The arrow indicates the position of  $\mu$  for  $B \rightarrow 0$ . (b) Solid (dotted) lines refer to calculations with self-consistency for every  $\eta$  (for  $\eta_0 = 9.5$  only).

$$\bar{n}_\nu(z) = n_\nu(z) / \int_0^\infty dz' n_\nu(z'),$$

to be approximately independent of  $B$ . Because the lowest two subbands are both heavy hole subbands,  $\bar{n}_1(z)$  and  $\bar{n}_2(z)$  differ appreciably. Now consider filling factors  $\eta \approx 17$ . We find that 15 ( $\eta - 2$ ) levels of the ground subband and that  $\eta - 15$  (2) levels of the first excited subband are occupied for  $\eta < 17$  ( $\eta > 17$ ). Thus, we have for the total density

$$n(z, \eta) \approx \begin{cases} N_h \left[ \frac{15}{\eta} \bar{n}_1(z) + \frac{\eta-15}{\eta} \bar{n}_2(z) \right], & \eta < 17 \\ N_h \left[ \frac{\eta-2}{\eta} \bar{n}_1(z) + \frac{2}{\eta} \bar{n}_2(z) \right], & \eta > 17, \end{cases}$$

and for its derivative  $dn/dB = xN_h[\bar{n}_1(z) - \bar{n}_2(z)]/(\eta B)$  with  $x = 15$  for  $\eta < 17$  and  $x = -2$  for  $\eta > 17$ , which explains the discontinuity in the derivative of the levels at  $\eta = 17$ .

On the other hand, at  $\eta \approx 18$ , the occupation of the ground (first excited) subband is  $\eta - 2$  (2) for  $\eta < 18$  and  $\eta > 18$  thus yielding no such discontinuity.

Although there are no discontinuities in the derivatives for the simplified calculation shown in Fig. 2(a), the distance between neighboring levels near the Fermi energy are almost the same as in Fig. 2(b), as can be seen by comparing the discontinuities of the Fermi energy in both figures.

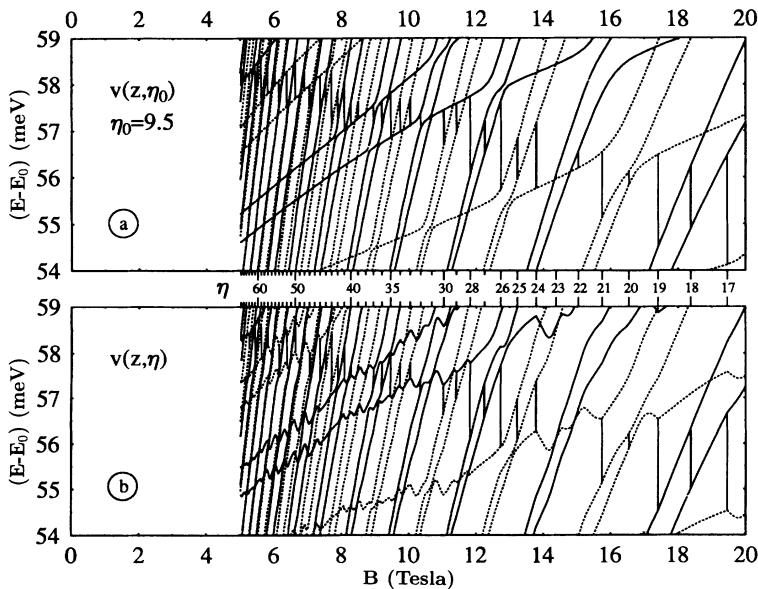


FIG. 2. Difference of Landau levels and the lowest level for an inversion layer with two occupied subbands ( $N_h = 8 \times 10^{12} \text{ cm}^{-2}$ ,  $N_d = 10^{15} \text{ cm}^{-3}$ ). Only the environment of the Fermi edge is shown. (a) Self-consistency only for  $\eta_0 = 9.5$ . (b) Self-consistency for every  $\eta$ .

### III. SHUBNIKOV–de HAAS EFFECT

In order to describe the Shubnikov–de Haas effect, one has to consider scattering by impurities with a potential  $v_i$ :

$$H = H_0 + V, \quad V(\mathbf{r}) = \sum_{i=1}^{N_i} v_i(\mathbf{r} - \mathbf{R}_i),$$

with the Hamiltonian of the impurity-free system  $H_0 = H_L + v(z)$ . Proceeding along the lines of Keiter,<sup>27</sup> we find for the full Green's function in the diagonal basis of  $H_0$ :

$$\mathcal{G}_{qjX, q'j'X'}(i\omega_n) = \delta_{XX'} \mathcal{G}_{qj, q'j'}(i\omega_n). \quad (6)$$

The Dyson equation runs in an obvious matrix notation [with  $\gamma = (q, j)$  as indices]:

$$\mathcal{G}(i\omega_n) = \mathcal{G}^{(0)}(i\omega_n) + \mathcal{G}^{(0)}(i\omega_n) \Sigma(i\omega_n) \mathcal{G}(i\omega_n), \quad (7)$$

with  $\mathcal{G}_{\gamma\gamma'}^{(0)}(i\omega_n) = \delta_{\gamma\gamma'}(i\omega_n - \xi_\gamma)^{-1}$  and  $\xi_\gamma = E_\gamma - \mu$ . In the self-consistent Born approximation (SCBA),<sup>28</sup> the self-energy runs

$$\Sigma_{\gamma_1\gamma_2} = \sum_{\gamma_3\gamma_4} \Gamma_{\gamma_1\gamma_2\gamma_3\gamma_4}^2 \mathcal{G}_{\gamma_3\gamma_4}, \quad (8)$$

$$\Gamma_{\gamma_1\gamma_2\gamma_3\gamma_4}^2 = \sum_{X'} \left\langle \sum_{i=1}^{N_i} \langle \gamma_1 X | v_i(\mathbf{r} - \mathbf{R}_i) | \gamma_3 X' \rangle \times \langle \gamma_4 X' | v_i(\mathbf{r} - \mathbf{R}_i) | \gamma_2 X \rangle \right\rangle_{\text{imp}}$$

As the problem given by Eqs. (6)–(8) is not feasible, we resort to the diagonal approximation,

$$\mathcal{G}_{\gamma_1\gamma_2}(i\omega_n) = \mathcal{G}_{\gamma_1} \delta_{\gamma_1\gamma_2}, \quad (9)$$

and evaluate  $\Gamma$  for a short-range potential  $v_i(\mathbf{r}) \sim \delta(\mathbf{r})$ . Then the elements  $\Gamma_{\gamma\gamma\gamma'\gamma'}$  differ only by a factor of up to 2 in the vicinity of the Fermi edge and we can approximate them by the constant  $\Gamma = \Gamma_0 \sqrt{B}$ , where  $\Gamma_0$  is independent of  $B$ .

Because of Eq. (9), the self-energy is diagonal and independent of the indices:

$$\Sigma(i\omega_n) = \Gamma^2 \sum_{\gamma} [i\omega_n - \xi_\gamma - \Sigma(i\omega_n)]^{-1}. \quad (10)$$

The density of states is

$$D(\xi, B) = \frac{1}{2\pi l^2} \sum_{\gamma} A_{\gamma}(\xi), \quad (11)$$

with the spectral function

$$A_{\gamma}(\xi) = -\frac{1}{\pi} \text{Im} \mathcal{G}_{\gamma}^R(\xi),$$

which is given by the *retarded* Green's function  $\mathcal{G}^R$  and

the Fermi energy  $\mu(B)$  is defined by

$$N_h = \int_{-\infty}^0 d\xi D(\xi, B). \quad (12)$$

When the distance  $\Delta E$  of the Landau levels is large against  $\Gamma$ , Eq. (10) results in the well-known semielliptic spectral function<sup>28</sup>  $A_{\gamma}^{(0)}(\xi)$ . In Fig. 3, we compare  $A_{\gamma}^{(0)}$  with the spectral function  $A_{\gamma}$ , which we get by solving Eq. (10) numerically, for a realistic example, where the condition  $\Delta E \gg \Gamma$  is violated and the Landau bands overlap. Obviously  $A_{\gamma}$  is much broader than  $A_{\gamma}^{(0)}$  and additionally has a number of local maxima, which are essential when calculating the conductivity. Also shown is the self-energy Eq. (10).

When summing in Eq. (10) over *all* levels, the series is not convergent. This is a consequence of our short-ranged potential  $v_i$ . For a finite-range potential  $v_i$ , the broadening  $\Gamma$  decreases with increasing  $j$  and this problem will not appear, but the self-energy would depend on  $\gamma$ . Thus, we sum in Eq. (10) only up to  $j_0$ . Then the self-energy depends on  $j_0$ , but we find numerically that a change of  $j_0$  leads only to a shift in the argument of the spectral function:  $A_{\gamma}^{(j_0)}(\xi) = A_{\gamma}^{(j'_0)}(\xi + \Delta\xi_{j_0j'_0})$ . Consequently, it is irrelevant which value for  $j_0$  we choose as the Fermi energy fixed by Eq. (12) is shifted likewise.

In SCBA, the evaluation of the conductivity is relatively simple. We neglect the particle-particle interaction. As the self-energy is independent of any quantum number, the vertex corrections vanish<sup>29</sup> and the transverse conductivity is

$$\sigma_{\mu\mu} = \frac{\pi}{V} \sum_{\gamma\gamma'} A_{\gamma}(0) A_{\gamma'}(0) |\langle \gamma | v_{\mu} \gamma' \rangle|^2.$$

The matrix elements of the velocity operator ( $v_x, v_y$ ) can easily be evaluated when exploiting that

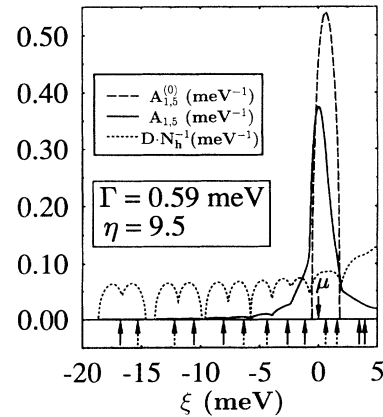


FIG. 3. Spectral function and density of states for an inversion layer with  $N_h = 2 \times 10^{12} \text{ cm}^{-2}$ ,  $N_d = 10^{15} \text{ cm}^{-3}$ ,  $\eta = 9.5$ , and  $\Gamma_0 = 0.2 \text{ meV T}^{-1/2}$ , i.e.,  $\Gamma = 0.59 \text{ meV}$ . For this broadening, the Landau levels overlap only partially. The arrows mark the position of the unbroadened Landau levels (cf. Fig. 1).

$$v_{\pm} = \mp \frac{1}{\sqrt{2}}(v_x \pm iv_y), \quad v_+ = l[a^\dagger, H], \quad v_- = l[a, H].$$

Because of the special structure of the eigenstates Eq. (5) the matrix elements  $\langle qj|v_\mu|q'j'\rangle$  vanish unless  $q \neq q'$ . Thus, in the Landau plot Fig. 1(a), two transitions are possible only between dotted and solid levels. As the Landau quantum number  $n$  is no good quantum number (especially for the highly excited states in the vicinity of the Fermi edge), there are no selection rules of the form  $n \rightarrow n \pm 1$  like for  $n$ -channel systems.

We find that  $\sigma_{yy}$  is about a factor of 2 larger than  $\sigma_{xx}$ , this factor being independent of  $B$ . The experimentally accessible quantity is the transversal resistivity  $\rho_{\mu\mu}$ , which is related to the conductivity by  $\rho_{xx} \sim B^2\sigma_{yy}$ ,  $\rho_{yy} \sim B^2\sigma_{xx}$  because  $\sigma_{xy} \gg \sigma_{xx}, \sigma_{yy}$  and  $\sigma_{xy} \sim B^{-1}$ . Shown in Fig. 4 are the resistivity for different hole densities and damping constants  $\Gamma_0$  (lower six curves) to-

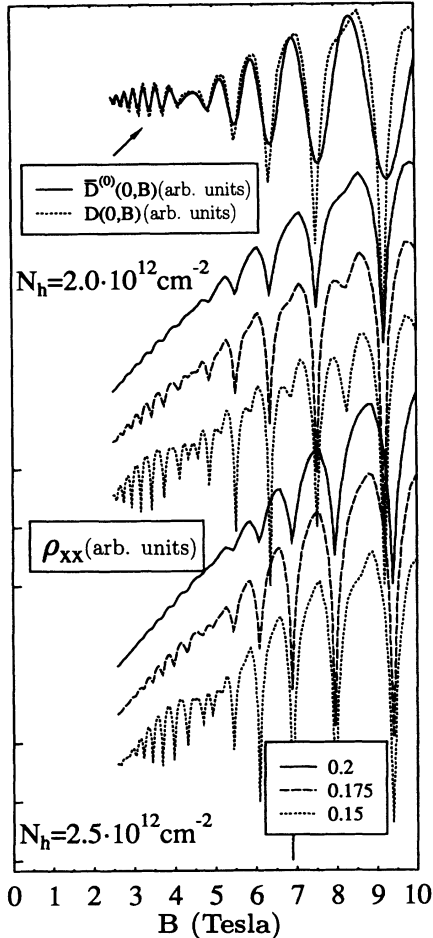


FIG. 4. Transversal resistivity  $\rho_{xx}$  (lower six curves) and density of states (upper two curves) for an inversion layer ( $N_d = 10^{15} \text{ cm}^{-3}$ ) with  $N_h = 2.0 \times 10^{12} \text{ cm}^{-2}$  (upper five curves) or  $N_h = 2.5 \times 10^{12} \text{ cm}^{-2}$ . The density of states is either in zeroth order LOCA ( $\bar{D}^{(0)}$  with  $\Gamma_0 = 0.2 \text{ meV T}^{-1/2}$ ) or in SCBA ( $D$  with  $\Gamma_0 = 0.3 \text{ meV T}^{-1/2}$ ). The resistivity has been calculated in SCBA with the broadening  $\Gamma_0/(\text{meV T}^{-1/2})$  given in the legend.

gether with the density of states  $D(0, B)$  Eq. (11) in SCBA and  $\bar{D}^{(0)}(0, B)$  in zeroth order of the LOCA (lowest order cumulant approximation).<sup>30</sup> In the latter case, the spectral function is

$$\bar{A}_\gamma^{(0)}(\xi) = \frac{1}{\sqrt{2\pi}\Gamma} e^{-(\xi-\xi_\gamma)^2/(2\Gamma^2)}, \quad (13)$$

with a Fermi energy defined by Eq. (12) evaluated with  $\bar{D}^{(0)}$  instead of  $D$ .

The resistivity curves reproduce well the measurements of von Klitzing *et al.* (Ref. 3, Fig. 1:  $N_h \approx 2.7 \times 10^{12} \text{ cm}^{-2}$ ). Obviously the essential information, i.e., the position of minima in the conductivity or the resistivity can be extracted from the density of states (upper curves), which can be calculated much easier than the conductivity. Especially the LOCA expression, Eq. (13), although being strictly valid only for  $\Delta E \gg \Gamma$  reproduces the minima of the conductivity without being required to solve an equation like (10) numerically. On the other hand, the corresponding density of states evaluated with the zeroth order expression  $A^{(0)}$  in SCBA would have unphysical structures.<sup>30</sup> Furthermore, the minima of the density of states and the conductivity in SCBA are too sharp. These are artifacts of the SCBA being absent in better approximations like the LOCA.

Figure 5 shows the density of states in LOCA for different densities  $N_h$  and doping concentrations  $N_d = 10^{15} \text{ cm}^{-3}$ . For low densities there are minima at odd filling factors  $\eta$  for high magnetic fields. In between is a beat (discovered by von Klitzing *et al.*<sup>3</sup>), a consequence of the spin-splitting of the subband structure for  $B = 0$  (a simple model is that of Bychkow and Rashba,<sup>31</sup> which cannot be applied here because of the anisotropy of the system). This behavior can be understood by considering the “discontinuities”  $\Delta\mu$  of the Fermi energy in Fig. 1. For integer  $\eta$ , the Fermi energy lies between the maxima of  $D(\xi, B)$  (considered to be a function of  $\xi$ ). Thus,  $D(0, B)$  (as a function of  $B$ ) has a minimum unless the highest occupied and the lowest unoccupied Landau level are very near each other: then the minimum will not appear, because two neighboring maxima in the self-energy [and thus in  $D(\xi, B)$ ] combine to a single maximum. In Fig. 1, we find that  $\Delta\mu$  is larger for  $\eta = 9, 11, 13$  than for  $\eta = 10, 12, 14$ . Consequently,  $\bar{D}^{(0)}(0, B)$  has minima for  $\eta = 9, 11, 13$ . For  $\eta \approx 18$ ,  $\Delta\mu$  is approximately equal for even and odd  $\eta$ . Thus, there is a beat at  $\eta \approx 18$ .

The position of the beat in dependence of  $N_h$  and  $N_d$  is summarized in Fig. 6. Obviously the doping concentration has only a weak influence on the position of the node. For  $N_d = 10^{15} \text{ cm}^{-3}$ , the Sham-Kohn result [Fig. 6(a)] reproduces well the experimental result by Dorozhkin and Ol’shanetskii,<sup>24</sup> whereas in the Hartree approximation [i.e., without the exchange-correlation contribution to  $v(z)$ ], the nodes are observed only in a limited density range and the agreement generally is worse than in the Sham-Kohn approximation.

When the second subband is occupied at higher densities  $N_h$ , the behavior of the Shubnikov-de Haas effect is even qualitatively changed. There is a second oscillation that can be explained by the oscillation of the discon-

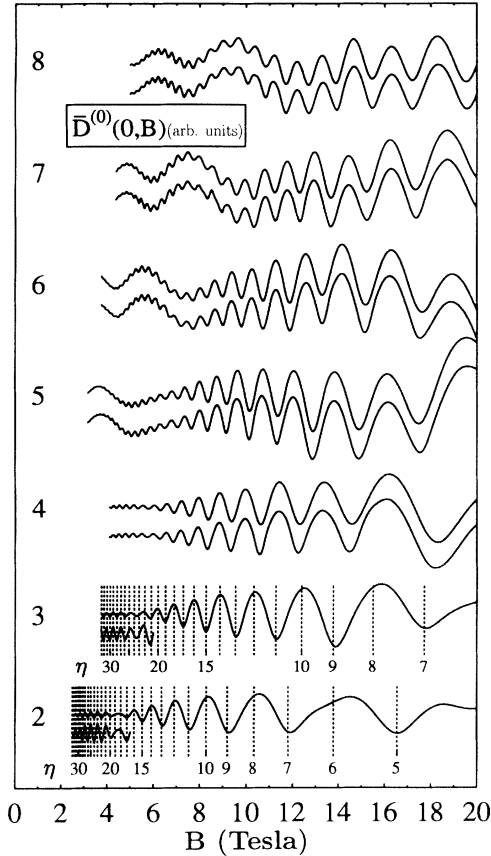


FIG. 5. Density of states for an inversion layer ( $N_d = 10^{15} \text{ cm}^{-3}$ ) with different hole densities [the numbers are  $N_h/(10^{12} \text{ cm}^{-2})$ ]. For only one occupied subband ( $N_h \leq 3 \times 10^{12} \text{ cm}^{-2}$ ) the curves additionally have been scaled up for large filling factors  $\eta$ . For two occupied subbands there are shown two curves for every  $N_h$ , the lower (upper) one referring to calculations with self-consistency for every  $\eta$  (only for  $\eta_0 = 9.5$ ).

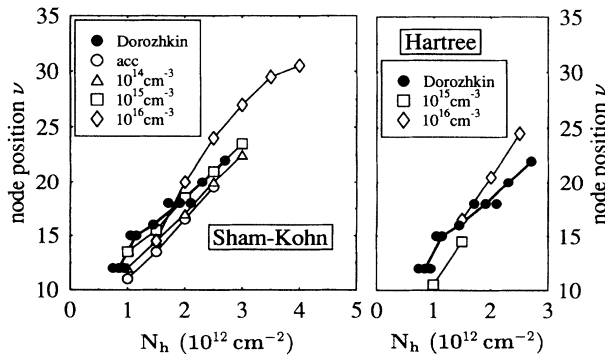


FIG. 6. Node position for an accumulation layer (acc) or an inversion layer with different doping concentrations  $N_d$  (given in the legend) and the corresponding result of Dorozhkin and Ol'shanetskii. (a) Sham-Kohn approximation. (b) Hartree result.

tinuity of the Fermi energy  $\Delta\mu$  at integer filling factors (see Fig. 2). The minima of  $\bar{D}^{(0)}(0, B)$  are *not* at integer filling factors  $\eta$  unless the damping is very small: then the zeroth order spectral functions do not overlap and the minima are at integer  $\eta$ . Usually, this is not the case in *p*-channel Si MOSFET's. Often the oscillations with a small period in  $B^{-1}$  are attributed to the ground subband and those with the large period in  $B^{-1}$  to the first excited subband. This interpretation requires that the occupation of a subband does not depend on  $B$ , which is the case as long as some levels of the higher subband are occupied as, e.g., for  $N_h = 8 \times 10^{12} \text{ cm}^{-2}$  (upper curve in Fig. 5): The Fourier transform  $H(f)$  of  $h(t) = \bar{D}^{(0)}(0, t^{-1})$  has two pronounced maxima at  $f_1 = 19.8 \text{ T}$  and  $f_2 = 142.5 \text{ T}$ , by which we can compute the population  $N_i = 2ef_i/h$  (SI) of the different subbands. Thus, we find a total concentration  $N_1 + N_2 = 7.85 \times 10^{12} \text{ cm}^{-2}$ , which differs only by 2% from  $N_h$ . The fraction of holes in the second subband is  $N_2/(N_1 + N_2) = 12.2\%$ . From the self-consistent calculation for  $B = 0$  (cf. Ref. 17), we find that 11.6% of the holes are in the second subband which within the error limits (only two periods of the second subband have been considered) verifies the statement that the surface density of different subbands can be determined by evaluating the different periods of the Shubnikov-de Haas oscillations.

Now we can compare with the experimental results of von Klitzing *et al.*,<sup>3</sup> who determined the position of the resistance maxima as a function of the gate voltage  $V_G$ . From this, we can extract (1) the fraction of holes in the second subband for large  $N_h$  (i.e., large  $V_G$ ) and (2) the critical concentration  $N_{hc}$  above which the second subband is populated. The latter is an indirect measure for the energetic distance of the two subbands: the larger this energy difference is, the larger is  $N_{hc}$ . In Fig. 7,  $N_2/N_h$  [or additionally  $(N_2 + N_3)/N_h$  when a third subband is populated] is shown as a function of

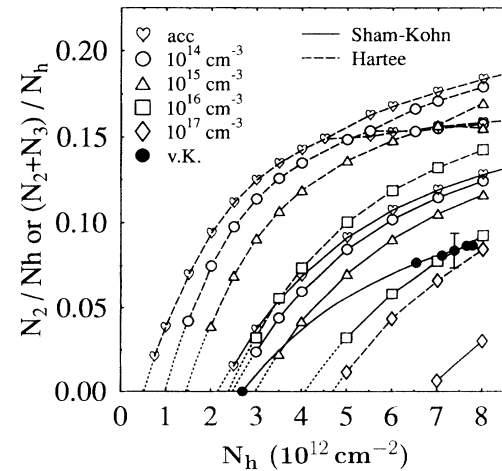


FIG. 7. Fraction of holes in the second or second and third subband for an accumulation layer (acc) or an inversion layer with different doping concentrations  $N_d$  (given in the legend) in the Sham-Kohn or the Hartree approximation together with the experimental result of von Klitzing *et al.*

$N_h$  for different doping concentrations  $N_d$  in Sham-Kohn and in the Hartree approximation (for simplicity the calculations are performed for  $B = 0$ ) as well as the experimentally found  $N_2/N_h$ . The critical concentration  $N_{hc}^{\text{exp}} = 2.7 \times 10^{12} \text{ cm}^{-2}$  is reproduced in the Sham-Kohn approximation for a plausible  $N_d$  between  $10^{14} \text{ cm}^{-3}$  and  $10^{15} \text{ cm}^{-3}$ , whereas in Hartree approximation unrealistically high doping concentrations between  $10^{16} \text{ cm}^{-3}$  and  $10^{17} \text{ cm}^{-3}$  are required. The theoretically found occupation of the second subband is too high, but in the Sham-Kohn approximation the curves are not as steep as in Hartree approximation, thus explaining the experiments better.

For the case of two occupied subbands, Fig. 5 shows two curves for every density, the lower one involving a self-consistent calculation of the Landau levels for every  $\eta$  and for the upper one the spectrum has been calculated with a potential  $v(z)$  determined self-consistently for  $\eta_0 = 9.5$ . There are only small differences concerning the large-period oscillations. Thus, it is sufficient to do the self-consistency only once for a large  $\eta_0$ .

#### IV. UNIAXIAL STRESS

When applying external stress  $\sigma_{\mu\nu}$  to the system, the Hamilton operator  $H_L$  (see the Appendix) and thus the subband structure and the Landau level spectrum are modified. Dorozhkin<sup>26</sup> experimentally applied a uniaxial stress  $\sigma_{\mu\nu} = \sigma_{xx}\delta_{\mu x}\delta_{\nu x}$  by bending the MOSFET. The corresponding strain tensor  $\varepsilon_{\mu\nu}$  can be found by inverting Hook's law  $\sigma = C\varepsilon$ . The nonvanishing components are  $\varepsilon_{xx}$ ,  $\varepsilon_{yy}$ ,  $\varepsilon_{zz}$ , which are related by

$$\varepsilon_{yy} = \varepsilon_{zz} = -\frac{C_{12}\varepsilon_{xx}}{C_{22} + C_{23}} = -\frac{C'_{12}\varepsilon_{xx}}{C'_{11} + C'_{12}}.$$

Here  $C_{ij}$  ( $C'_{ij}$ ) are elastic constants in the nontensorial Voigt notation<sup>32</sup> for a coordinate system with  $\hat{z} = [110]$ ,  $\hat{x} = [00\bar{1}]$ ,  $\hat{y} = [\bar{1}10]$  ( $\hat{x}' = [100]$ ,  $\hat{y}' = [010]$ ,  $\hat{z}' = [001]$ ). By such a uniaxial stress, the symmetry at a  $[110]$  surface in a perpendicular magnetic field is not reduced: the symmetry group is  $C_2$ , even if  $\varepsilon_{xx} \neq 0$ . We use the parameters<sup>32</sup>  $D_u = 2.88 \text{ eV}$ ,  $D'_u = 4.42 \text{ eV}$ ,  $C'_{11} = 169 \text{ GPa}$ ,  $C'_{12} = 65 \text{ GPa}$  (the latter two for  $T = 4 \text{ K}$ ) and for the doping concentration we choose  $N_d = 10^{15} \text{ cm}^{-3}$  as this explains the node position for  $\varepsilon_{xx} = 0$  best (see Sec. III).

The main effect of the deformation is a shift of the node position shown in Fig. 8 along with the experimental results of Dorozhkin.<sup>26</sup> In case of compression ( $\varepsilon_{xx} < 0$ ), we found the beat to be shifted to lower filling factors  $\eta$  and at low concentrations  $N_h$  an additional node emerges at large  $\eta$ . In case of expansion ( $\varepsilon_{xx} > 0$ ), the beat is shifted to higher  $\eta$  and an additional node appears at small  $\eta$ , which is almost independent of  $N_h$  and  $\varepsilon_{xx}$ . Experimentally, Dorozhkin found only one node, which depends almost linearly on  $\varepsilon_{xx}$ , whereas our calculations predict a saturation already for  $|\varepsilon_{xx}| = 3 \times 10^{-3}$ . For high concentrations  $N_h$  the slope of  $\nu(\varepsilon_{xx})$  is only poorly reproduced.

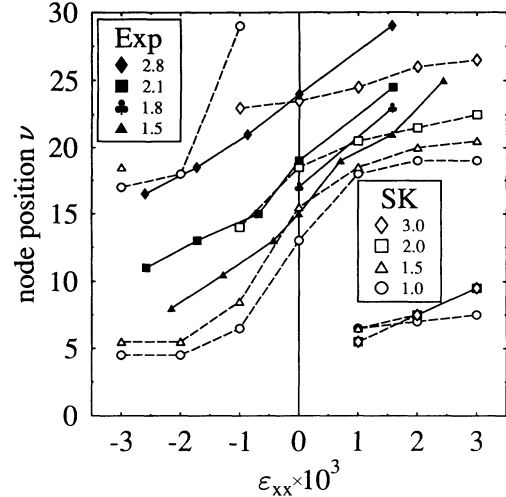


FIG. 8. Filling factor  $\nu$  at which a node appears in the magnetoquantum oscillations as a function of the strain  $\varepsilon_{xx}$ . The calculations in the Sham-Kohn approximation (SK) are performed for an inversion layer with  $N_d = 10^{15} \text{ cm}^{-3}$ . The experimental results are by Dorozhkin. The numbers in the legends are the hole concentration  $N_h/(10^{12} \text{ cm}^{-2})$ .

Possible reasons for this discrepancy are (1) calibration of stress experiments is difficult. An error of 50% for  $\varepsilon_{xx}$  is possible, but rescaling the  $\varepsilon_{xx}$  axis alone cannot explain the discrepancy. (2) In order to investigate the dependence on the deformation potentials, we tried another set of parameters ( $D_u = 3.40 \text{ eV}$ ,  $D'_u = 4.42 \text{ eV}$ ):<sup>32</sup> As long as only one subband is populated, the density of states is almost unchanged. The deformation potentials have an influence on how much the second subband is populated with increasing  $N_h$ , but do not change the position of the node for two occupied subbands. Thus, the influence of  $D_u$ ,  $D'_u$  seems to be uncritical. (3) Therefore, besides possible calibration errors the uncertainty of the Luttinger parameters is expected to be the main cause of the discrepancy between theoretical and experimental results.

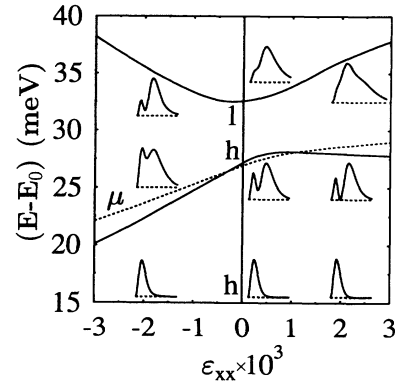


FIG. 9. Energy difference between excited bands and the ground subband for  $k = 0$  ( $B = 0$ ) as a function of the strain  $\varepsilon_{xx}$  for an inversion layer with  $N_h = 3 \times 10^{12} \text{ cm}^{-2}$ ,  $N_d = 10^{15} \text{ cm}^{-3}$ . The insets show the square of the corresponding wave functions  $|\chi(z)|^2$  for  $\varepsilon_{xx} = 0$  and  $\varepsilon_{xx} = \pm 2 \times 10^{-3}$ .

The uniaxial strain also has an influence on the relative energetic position of the subband edges. This is shown for an inversion channel with  $N_h = 3 \times 10^{12} \text{ cm}^{-2}$ ,  $N_d = 10^{15} \text{ cm}^{-3}$  in Fig. 9. For  $|\varepsilon_{xx}| \gtrsim 10^{-3}$  the second subband is populated. Whether the second and third subbands are heavy or light holelike depends on  $\varepsilon_{xx}$ . However, for large  $|\varepsilon_{xx}|$  a distinction between heavy and light holes is almost impossible for the excited subbands. In Fig. 9 the square  $|\zeta(z)|^2$  of the wave functions at  $k = 0$  has been indicated. Whereas, for  $\varepsilon_{xx} \geq 0$ , the third subband is ground state like, for  $\varepsilon_{xx} \lesssim -10^{-3}$  the second subband is about ground state like. For finite  $\mathbf{k}$ , the situation is much more complicated.

## V. SUMMARY

We investigated  $p$ -type accumulation and inversion layers at a [110]-Si surface in large external magnetic fields in Sham-Kohn approximation. When only one subband is occupied, the Hartree and the exchange-correlation potential, which have to be determined self-consistently, are almost independent of the magnetic field unless the system is in the magnetic quantum limit. On the other hand, there is a definite dependence of the potential on the magnetic field when a second subband is populated, leading to discontinuities of the slope of the Landau levels at certain integer filling factors.

The Shubnikov-de Haas effect, i.e., the transversal resistivity of the quasi-two-dimensional hole system, has been calculated in SCBA. It has been shown that the position of the minima is the same as for the density of states at the Fermi edge, which can be calculated easily in zeroth order LOCA. We could reproduce the density dependence of the beating pattern in the magnetoquantum oscillations. In the Sham-Kohn approximation, we could explain the critical concentration  $N_{hc}$  above which the second subband is populated, in Hartree approximation we could not. The former approximation yields somewhat too large concentrations for the holes in the second subband when the density  $N_h$  is increased above  $N_{hc}$ , but these values are better than the corresponding Hartree result.

For the MOSFET under uniaxial stress, we investigated the strain dependence of the node position  $\nu(\varepsilon_{xx})$ . The slope of this curve could be reproduced within a factor of 2. The discrepancy is mainly attributed to uncertainties in the Luttinger parameters.

## ACKNOWLEDGMENTS

I am grateful to Professor G. Landwehr, who supported this work as the head of the Graduiertenkolleg "Mikrostrukturierte Halbleiter," as well as to Dr. E. Bangert and V. Latussek for many valuable discussions.

## APPENDIX

We explicitly write down Luttinger's matrix  $H_L$  because (1) we choose a special coordinate system ( $\hat{\mathbf{z}}$  =

[110],  $\hat{\mathbf{x}} = [00\bar{1}]$ ,  $\hat{\mathbf{y}} = [\bar{1}10]$ ) and (2) sometimes the term being explicitly  $\mathbf{B}$  dependent is given wrong in the literature (e.g., in Ref. 33). It consists of a term  $H_0$ , which is independent of the external fields, of an explicitly  $\mathbf{B}$ -dependent term  $H_B$  and finally of  $H_\varepsilon$ , which depends on an external strain  $\varepsilon_{\mu\nu}$ :<sup>33,34</sup>

$$H_L(\mathbf{k}', \mathbf{B}, \varepsilon_{\mu\nu}) = H_0(\mathbf{k}') + H_B(\mathbf{B}) + H_\varepsilon(\varepsilon_{\mu\nu}). \quad (\text{A1})$$

$H_0(\mathbf{k}')$  is the matrix  $\bar{H}_0(\mathbf{k}')$  given in Ref. 17, which has been unitarily transformed:

$$H_0 = \mathcal{D} \bar{H}_0 \mathcal{D}^\dagger, \quad (\text{A2})$$

$$\mathcal{D} = \text{diag}(\alpha^3, \alpha, \alpha^{-1}, \alpha^{-3}, \alpha, \alpha^{-1}), \quad \alpha = e^{i\pi/4},$$

in order to achieve a real matrix for finite  $\mathbf{B}$ .  $\bar{H}_0$  and, thus,  $H_0$  can be written in terms of the operators  $A_\pm$ ,  $B$ ,  $C$ ,  $D$ , and  $A = H_2$ , which are functions of  $a$ ,  $a^\dagger$ ,  $N$ , and  $k_z$ :

$$A_\pm = \left( 1 \mp \frac{3\gamma_3 + \gamma_2}{2\gamma_1} \right) k_z^2 + \frac{1}{l^2} \left( 1 \pm \frac{3\gamma_3 + \gamma_2}{4\gamma_1} \right) (2N + 1) \mp \frac{3}{4l^2} \frac{\gamma_3 - \gamma_2}{\gamma_1} (a^{\dagger 2} + a^2),$$

$$A = k_z^2 + \frac{1}{l^2} (2N + 1) + \Delta,$$

$$B = -\frac{\sqrt{6}}{l} \left[ \frac{\gamma_3 - \gamma_2}{\gamma_1} a^\dagger + \frac{\gamma_3 + \gamma_2}{\gamma_1} a \right] \cdot ik_z,$$

$$C = \frac{\sqrt{3}}{2} \frac{\gamma_3 - \gamma_2}{\gamma_1} k_z^2 - \frac{\sqrt{3}}{4l^2} \frac{\gamma_3 - \gamma_2}{\gamma_1} (2N + 1) - \frac{3\sqrt{3}}{4l^2} \frac{\gamma_3 - \gamma_2}{\gamma_1} a^{\dagger 2} + \frac{\sqrt{3}}{4l^2} \frac{5\gamma_3 + 3\gamma_2}{\gamma_1} a^2,$$

$$D = \frac{1}{\sqrt{2}} (A_+ - A_-).$$

When considering the spherical symmetric term  $H_B$ , we have to take care of the electron spin. Luttinger's result (in SI units)

$$\hat{H}_B = -(3\kappa + 1)\mu_B \mathbf{B} \cdot \mathbf{I} + \mu_B \mathbf{B} \cdot \boldsymbol{\sigma},$$

yields after transformation to our  $j = \frac{3}{2}, \frac{1}{2}$  basis with  $U = \langle 1m_l, \frac{1}{2}m_s | jm_j \rangle$  (in effective units):

$$\bar{H}_B = U^\dagger \hat{H}_B U = \begin{pmatrix} 2 \frac{\kappa}{\gamma_1} \mathbf{B} \cdot \mathbf{J} & 3 \frac{\kappa+1}{\gamma_1} \mathbf{B} \cdot \mathbf{T}^\dagger \\ 3 \frac{\kappa+1}{\gamma_1} \mathbf{B} \cdot \mathbf{T} & 2 \frac{\kappa+1}{\gamma_1} \mathbf{B} \cdot \boldsymbol{\sigma} \end{pmatrix},$$

where  $\mathbf{I}$ ,  $\mathbf{J}$ ,  $\boldsymbol{\sigma}$  are three-, four- and two-dimensional representations of the angular momentum operator corresponding to spin 1, 3/2, and 1/2 and the matrices  $\mathbf{T}$  are given in Ref. 33. We assume Luttinger's parameter  $\mathbf{q}$  to be zero. As a result of  $\mathbf{k} \cdot \mathbf{p}$  perturbation theory,  $\kappa$  is related to  $\gamma_1, \gamma_2, \gamma_3$  by<sup>33</sup>

$$\gamma_1 - 2\gamma_2 - 3\gamma_3 + 3\kappa + 2 = 0.$$

The term depending on  $\varepsilon_{\mu\nu}$  is found to be<sup>33</sup>

$$\begin{aligned}\hat{H}_\varepsilon = & D_d^v \text{Tr} \varepsilon + 2D_u [(I_x^2 - I^2/3) \varepsilon_{xx} + \text{c.p.}] \\ & + 4D'_u [\{I_x I_y\} \varepsilon_{xy} + \text{c.p.}] \\ & + (D_u - D'_u) [-(I_y^2 - I_z^2) (\varepsilon_{yy} - \varepsilon_{zz}) \\ & + 4\{I_y I_z\} \varepsilon_{yz}],\end{aligned}$$

$$\bar{H}_\varepsilon = U^\dagger \hat{H}_\varepsilon U, \quad \{AB\} = (AB + BA)/2$$

with the deformation potentials  $D_d^v$  (irrelevant in our case),  $D_u, D'_u$ . Finally,  $\bar{H}_B$  and  $\bar{H}_\varepsilon$  have to be transformed according to Eq. (A2).

- 
- <sup>1</sup> T. Ando, A. B. Fowler, and F. Stern, *Rev. Mod. Phys.* **54**, 437 (1982).  
<sup>2</sup> T. Ando, *J. Phys. Soc. Jpn.* **51**, 3893 (1982).  
<sup>3</sup> K. von Klitzing, G. Landwehr, and G. Dorda, *Solid State Commun.* **14**, 387 (1974).  
<sup>4</sup> K. von Klitzing, G. Landwehr, and G. Dorda, *Solid State Commun.* **15**, 489 (1974).  
<sup>5</sup> K. von Klitzing, G. Landwehr, and G. Dorda, *Proceedings of the 2nd International Conference on Solid Surfaces, 1974* [*Jpn. J. Appl. Phys. Suppl.* **2**, Pt. 2, 351 (1974)].  
<sup>6</sup> G. Landwehr, E. Bangert, K. von Klitzing, Th. Englert, and G. Dorda, *Solid State Commun.* **19**, 1031 (1976).  
<sup>7</sup> J. M. Luttinger and W. Kohn, *Phys. Rev.* **97**, 869 (1955).  
<sup>8</sup> J. M. Luttinger, *Phys. Rev.* **102**, 1030 (1956).  
<sup>9</sup> V. Latussek, E. Bangert, and G. Landwehr, *Ann. Phys. (Leipzig)* **48**, 394 (1991).  
<sup>10</sup> E. Bangert, K. von Klitzing, and G. Landwehr, *Proceedings of the Twelfth International Conference on the Physics of Semiconductors, Stuttgart, 1974* (Teubner, Stuttgart, 1974), p. 714.  
<sup>11</sup> E. Bangert and G. Landwehr, *Surf. Sci.* **58**, 138 (1976).  
<sup>12</sup> F. J. Ohkawa and Y. Uemura, *Prog. Theor. Phys. Suppl.* **57**, 164 (1975).  
<sup>13</sup> D. A. Broido and L. J. Sham, *Phys. Rev. B* **34**, 3917 (1986).  
<sup>14</sup> Y. Iwasa, N. Miura, S. Tarucha, H. Okamoto, and T. Ando, *Surf. Sci.* **170**, 587 (1986).  
<sup>15</sup> U. Ekenberg, *Phys. Rev. B* **38**, 12 664 (1988).  
<sup>16</sup> E. Bangert and G. Landwehr, *Surf. Sci.* **170**, 593 (1986).  
<sup>17</sup> W. O. G. Schmitt, preceding paper, *Phys. Rev. B* **50**, 15 221 (1994).  
<sup>18</sup> L. J. Sham and W. Kohn, *Phys. Rev.* **145**, 561 (1966).  
<sup>19</sup> T. Ando, *Phys. Rev. B* **13**, 3468 (1976).  
<sup>20</sup> P. Hohenberg and W. Kohn, *Phys. Rev.* **136**, B864 (1964).  
<sup>21</sup> W. Kohn and L. J. Sham, *Phys. Rev.* **140**, A1133 (1965).  
<sup>22</sup> R. M. Dreizler and E. K. U. Gross, *Density Functional Theory* (Springer-Verlag, Berlin, 1990).  
<sup>23</sup> G. Vignale and M. Rasolt, *Phys. Rev. B* **37**, 10 685 (1988).  
<sup>24</sup> S. I. Dorozhkin and E. B. Ol'shanetskii, *Sov. Phys. Usp.* **46**, 399 (1987) [*JETP Lett.* **46**, 502 (1987)].  
<sup>25</sup> S. I. Dorozhkin, *Solid State Commun.* **72**, 211 (1989).  
<sup>26</sup> S. I. Dorozhkin (unpublished).  
<sup>27</sup> H. Keiter, *Z. Phys.* **198**, 215 (1967).  
<sup>28</sup> T. Ando and Y. Uemura, *J. Phys. Soc. Jpn.* **36**, 959 (1974).  
<sup>29</sup> R. Gerhardt and J. Hajdu, *Z. Phys.* **245**, 126 (1971).  
<sup>30</sup> R. Gerhardt, *Z. Phys. B* **21**, 285 (1975).  
<sup>31</sup> Y. A. Bychkov and E. I. Rashba, *Sov. Phys. Usp.* **146**, 632 (1985) [*JETP Lett.* **39**, 78 (1984)].  
<sup>32</sup> M. Cardona, O. Madelung, G. Habeke, and U. Rössler, in *Semiconductors. Physics of Group IV Elements and III-V Compounds*, edited by O. Madelung, Landolt-Börnstein, New Series, Group 3, Vol. 17, Pt. a (Springer, Berlin, 1982), p. 43.  
<sup>33</sup> H.-R. Trebin, U. Rössler, and R. Ranvaud, *Phys. Rev. B* **20**, 686 (1979).  
<sup>34</sup> G. L. Bir and G. E. Pikus, *Symmetry and Strain-Induced Effects in Semiconductors* (Wiley, Chichester, 1974).